HHS Public Access

Author manuscript

Dev Biol. Author manuscript; available in PMC 2016 March 15.

Published in final edited form as:

Dev Biol. 2015 March 15; 399(2): 283–295. doi:10.1016/j.ydbio.2015.01.004.

RhoGAP68F controls transport of adhesion proteins in Rab4 endosomes to modulate epithelial morphogenesis of *Drosophila* leg discs

Beatriz Hernandez de Madrid, **Lina Greenberg**, and **Victor Hatini***

Department of Developmental, Molecular and Chemical Biology, Program in Cell, Molecular and Developmental Biology, Program in Genetics, Sackler School of Graduate Biomedical Sciences, Tufts University School of Medicine, 150 Harrison Avenue, Boston MA 02111

SUMMARY

Elongation and invagination of epithelial tissues are fundamental developmental processes that contribute to the morphogenesis of embryonic and adult structures and are dependent on coordinated remodeling of cell-cell contacts. The morphogenesis of *Drosophila* leg imaginal discs depends on extensive remodeling of cell contacts and thus provides a useful system with which to investigate the underlying mechanisms. The small Rho GTPase regulator RhoGAP68F has been previously implicated in leg morphogenesis. It consists of an N-terminal Sec14 domain and a C-terminal GAP domain. Here we examined the molecular function and role of RhoGAP68F in epithelial remodeling. We find that depletion of RhoGAP68F impairs epithelial remodeling from a pseudostratified to simple, while overexpression of RhoGAP68F causes tears of lateral cell-cell contacts and thus impairs epithelial integrity. We show that the RhoGAP68F protein localizes to Rab4 recycling endosomes and forms a complex with the Rab4 protein. The Sec14 domain is sufficient for localizing to Rab4 endosomes, while the activity of the GAP domain is dispensable. RhoGAP68F, in turn, inhibits the scission and movement of Rab4 endosomes involved in transport the adhesion proteins Fasciclin3 and E-cadherin back to cell-cell contacts. Expression of RhoGAP68F is upregulated during prepupal development suggesting that RhoGAP68F decreases the transport of key adhesion proteins to the cell surface during this developmental stage to decrease the strength of adhesive cell-cell contacts and thereby facilitate epithelial remodeling and leg morphogenesis.

Keywords

Epithelial morphogenesis; leg imaginal disc; tarsus; Rho GTPases; endocytic trafficking; Rab5; Rab4; Rab7; E-cadherin; Fasciclin3

*Corresponding author: Tel.: +1 617 636 3493; Fax: +1 617 636 3676. victor.hatini@tufts.edu (V. Hatini).

INTRODUCTION

Epithelial tissues form cohesive sheets and play critical roles in processes such as the covering of internal and external surfaces and the regulation of surface and trans-epithelial transport. During development epithelial sheets undergo extensive remodeling to elaborate the shape of the embryo and its constituent tissues and organs. This remodeling is mediated by coordinated tissue-level changes in cell proliferation, cell death, cell shape and rearrangements of cell contacts (Gumbiner, 2005). The adherens junctions (AJs) underlie the property of epithelial tissues to remodel tissue shape while maintaining tissue cohesion. The AJs form a belt-like structure below the apical surface of the epithelium (Takeichi, 2014) composed of the single pass transmembrane protein E-cadherin (E-cad) and associated components (Oda et al., 1994; Tepass et al., 1996). E-cad molecules are dynamically endocytosed and recycled back to the cell surface providing epithelial cells with the plasticity to dynamically rearrange cell shape and cell-cell contacts (Georgiou et al., 2008; Harris and Tepass, 2008; Leibfried et al., 2008). The septate junctions (SJs), which contribute to the barrier function of the epithelium, assemble below the AJs and consist of membrane attachment sites and septa that give the junctions a ladder-like appearance (Tepass & Hartenstein, 1994). The composition of the SJs is complex and consists of at least fifteen transmembrane proteins that can be subdivided into several functional groups (Oshima and Fehon, 2011). One functional group contributes to the barrier function of the epithelium (Genova and Fehon, 2003). Other groups of SJs proteins are required to establish or maintain epithelial apicobasal polarity (Bilder et al., 2000; Laprise et al., 2009). The roles of other SJs proteins such as the immunoglobulin superfamily members Fasciclin2 (Fas2) and Fasciclin3 (Fas3) are just being elucidated (Gomez et al., 2012; Wells et al., 2013). Mechanisms affecting SJs dynamics and the contribution of this dynamics to tissue morphogenesis are poorly understood.

The dynamic association of the AJs with networks of actin filaments drives many morphogenetic events such as tissue bending and elongation by affecting cell shape and rearrangements of cell contacts, respectively (Bertet et al., 2004; Blankenship et al., 2006; Cavey et al., 2008; Levayer and Lecuit, 2013; Martin et al., 2009). Contraction of actomyosin networks, and the transmission of tensile forces to the cell surface by the coupling of these networks to the AJs, transiently deform cell-cell contacts and cell shape (reviewed in) (Guillot and Lecuit, 2013; Heisenberg and Bellaiche, 2103). The remodeling of cell contacts and the acquisition of new cell shapes require stabilization of these transient deformations through the regulation of the amount and dynamics of junctional proteins at the cell surface (Wirtz-Peitz and Zallen, 2009). The surface expression of adhesion proteins reflects a balance between endocytic internalization, recycling and lysosomal degradation affecting the strength of adhesive cell-cell contacts (Delva and Kowalczyk, 2009; Yap et al., 2007). The modulation of this balance can stabilize transient deformations at the cell surface by insertion or removal of membrane and adhesion receptors to or from the cell surface, respectively. The modulation of endocytic trafficking routes have been implicated in remodeling of epithelial cell shape in various morphogenetic processes including apical constriction (Lee and Harland, 2010), cell intercalation (Levayer et al., 2011; Shaye et al., 2008), dorsal closure (Mateus et al., 2011), and planar cell polarity (Classen et al., 2005;

Warrington et al., 2013). However the precise mechanisms regulating endocytic internalization, recycling and degradation of adhesion receptors during epithelial remodeling remain poorly understood.

Small Rab GTPases regulate vesicle transport along the different transport routes and thereby the abundance and dynamics of adhesive contacts at the cell surface (Maxfield and McGraw, 2004; Stenmark, 2009). Key Rab regulators of endocytic trafficking include Rab5, 4, 7 and 11. Rab5 regulates the transport of cargo in primary vesicles to early endosomes that function as primary sorting stations in the endocytic pathway (Bucci et al., 1992), Rab4 the direct return of cargo to the cell surface from early endosomes (van der Sluijs et al., 1992), Rab11 the slow recycling of cargo to the cell surface (Chen et al., 1998; Ren et al., 1998), and Rab7 the transport of cargo to late endosomes for degradation in lysosomes or the trans-Golgi for later use (Bucci et al., 2000; Press et al., 1998; Vitelli et al., 1997). Small Rho GTPases also regulate endocytic trafficking (Ridley, 2006). The small Rho GTPase Cdc42 promotes endocytic internalization from the cell surface (Georgiou et al., 2008; Harris and Tepass, 2008; Leibfried et al., 2008), and vesicle movement inside the cell through the regulation of the actin nucleation promoting factors (NPFs) WASP and WAVE (Fricke et al., 2009). In addition, the NPF WASH and its putative Rho GTPase regulator control scission and movement of vesicles in the endocytic compartment (Derivery et al., 2009; Gomez and Billadeau, 2009). Small Rho and Rab GTPases are thought to function as platforms for the recruitment of proteins that regulate key steps in vesicle transport such as vesicle formation, budding, scission, movement, targeting and fusion with a target compartment. However, the upstream regulators of Rab and Rho GTPases along the different endocytic routes are largely unknown, nor the role of these regulators in control of epithelial tissue morphogenesis.

RhoGAP68F consists of an N-terminal Sec14 domain, an N-terminal GAP domain and an intervening proline-rich region. Most Sec14-only proteins regulate phospholipid transfer between membrane compartments to control organalle physiology and determine the outcomes of phosophoinositide signaling (Bankaitis et al. 2010; Curwin et al., 2009; Saito et al., 2007; Schaaf et al., 2008). Several modular Sec14 proteins that contain one or more GAP or GEF domain/s were found to participate in regulation of endosome dynamics and intracellular vesicle traffic *in vitro* (Sirokmany et al., 2006; Sun et al., 2006). RhoGAP68F was previously found to affect gastrulation and was proposed to modulate apical constriction through regulation of actomyosin contractility. However, neither the subcellular localization nor the molecular function of the protein were determined (Sanny et al., 2006). In the leg imaginal disc, depletion or overexpression of *RhoGAP68F* function impair the morphology of the distal tarsus without adversely affecting tarsus segmentation suggesting a role for the protein in epithelial remodeling (Greenberg and Hatini, 2011).

Here we investigated the mechanism of RhoGAP68F function and its role in epithelial remodeling. We show that RhoGAP68F physically interacts with and localizes to Rab4 endosomes, which we find transport Fas3 and E-cad back to the cell surface from early endosomes. The N-terminal Sec14 domain of RhoGAP68F is sufficient to localize to the Rab4 compartment, while the activity of the C-terminal GAP domain is not required. RhoGAP68F, in turn, inhibits the scission and movement of the Rab4 endosomes back to the

cell surface. We provide evidence that through inhibition of an entire endocytic organelle engaged in transport adhesion proteins back to the cell surface, RhoGAP68F decreases the strength of adhesive cell-cell contacts to facilitate epithelial elongation and invagination at presumptive joints.

RESULTS

(A) Elongation of the leg epithelium coincides with planar and apicobasal cell rearrangements

During the early stages of pupal development (2–6h APF) cells in the epithelium of the *Drosophila* leg imaginal disc change shape (Condic et al., 1991; Greenberg and Hatini, 2011; Mirth and Akam, 2002; Tajiri et al., 2011), and rearrange contacts with their neighbors (Taylor and Adler, 2008), to narrow and so elongate and the future appendage (von Kalm et al., 1995). To examine the rearrangements of the epithelium along the apicobasal axis, we labeled nuclei with Dapi and the lateral membrane domain with Fas3 (Fig. 1A–C). At 2 hours APF, the epithelium was largely pseudostratified as cell nuclei were found at different positions along the apicobasal axis. An exception was observed in the ventral region of tarsal segments t3–t4 where the epithelium was mostly simple and associated with presumptive joints that were already folded (Fig. 1A). At 4h APF the epithelium became mostly simple as nuclei moved relative to each other to form a single layer except for parts of t1 and t5 that remained pseudostratified (Fig. 1B). By 6h APF the epithelium assumed mostly a simple morphology (Fig. 1C). Thus, during early prepupal stages, the pseudostratified epithelium of the leg imaginal disc becomes progressively simpler.

(B) Depletion or overexpression of RhoGAP68F impair the planar and apicobasal rearrangements of the epithelium

To better understand the cellular processes involved in epithelial elongation, we examined the planar and apicobasal organization of the epithelium of prepupal legs with reduced or elevated levels of RhoGAP68F. We used two distinct partially overlapping RhoGAP68F RNAis that successfully depleted the RhoGAP68F protein in imaginal discs and yielded similar leg phenotypes (Supplemental Fig. 1A–B) (Dietzl et al., 2007; Ni et al., 2009; Greenberg and Hatini, 2011). We found that the apical profiles of epithelial cells in *RhoGAP68F* depleted legs were uniformly small, in contrast to the constricted and expanded apical profiles at presumptive joints and segments, respectively, in wild type (Supplemental Fig. 2) (Greenberg and Hatini, 2011). Additionally, the transition of epithelial morphology from a pseudostratified to simple was also impaired (Fig. 1D–F). Thus, depletion of *RhoGAP68F* impaired both the planar and apicobasal organization of the leg epithelium.

To examine the effect of RhoGAP68F over expression on epithelial organization, we generated several UAS lines by P-element-mediated insertion. To judge the strength of these insertions, we crossed each of these UAS lines to the *Dll-GAL4* driver to express RhoGAP68F in the distal part of the leg. We scored the resulting morphological defects in adult legs and identified three classes referred to as weak, moderate and strong. The expression of RhoGAP68F from weak insertions had no effect on the morphology of adult

legs. These insertions were used to map the subcellular localization of the RhoGAP68F protein as described below. Expression of RhoGAP68F from strong insertions led to pupal lethality and necrosis of the tarsus that precluded the analysis of epithelial morphology (data not shown). Expression of RhoGAP68F from moderate insertions impaired the morphology of the tarsal region, and led to low incidence of broken tarsi (data not shown). Analysis of prepupal legs revealed tears in the epithelium, proximal to the nascent tarsal joints (4/33 discs analyzed; arrows Fig. 1G). These tears formed below the AJs and SJs and above the basal surface of the epithelium along the lateral membrane domain. Interestingly, Fas3 accumulated at high levels in the proximal part of tarsal segments (arrows in Fig. 1B–C) that were prone to tear (arrows in Fig. 1G–H).

Taken together, these studies suggest that optimal levels of RhoGAP68F are required for proper morphogenesis of the prepupal leg epithelium.

(C) mCherry-RhoGAP68F localizes preferentially to Rab4 endosomes

To understand how RhoGAP68F affects the planar and apicobasal rearrangements of the epithelium, we tagged RhoGAP68F with a mCherry (mC) fluorescent protein and examined the subcellular distribution of the tagged protein in the leg epithelium. We found that a weak *UAS-mC-RhoGAP68F* expressed in the distal part of the leg disc localized to punctate structures in the cytoplasm (Fig. 2A). To determine if these structures where endocytic, we labeled the lumen of newly formed endosomes *ex vivo* in dissected leg discs by the uptake of fluorescent dextran by fluid phase endocytosis (10 min pulse followed by 20 min chase to visualize early endosomes; Entchev et al., 2000). We found that a subset of the mC-RhoGAP68F puncta colocalized with the fluorescent dextran in newly formed endosomes (Fig. 2B). To determine the subcellular site of action of RhoGAP68F in the endocytic pathway, we examined the localization of mC- RhoGAP68F relative to Rab5 and Rab4 early endosomes, Rab11 recycling endosomes, and Rab7 late endosomes. We co-expressed the mC-RhoGAP68F protein with each Rab protein tagged with YFP (Zhang et al., 2007), or GFP (Entchev et al., 2000; Wucherpfennig et al., 2003), and examined mC-RhoGAP68F localization relative to each endocytic compartment (Fig. 2C–F). The localization of the tagged Rab proteins appeared to largely recapitulate the localization of the endogenous proteins (compare Supplemental Fig. 3 to Supplemental Fig. 4). However, expression of the tagged Rab proteins led to a slight enlargement of vesicles that aided in their identification in agreement with the original report describing the collection of the YFP-Rab proteins (Supplemental Fig. 1C, and Supplemental Fig. 3) (Zhang et al., 2007). Importantly, expression of each of the tagged Rab proteins alone had no affect on the morphology of the tarsal region. We found that mC-RhoGAP68F co-localized moderately with the Rab5-GFP early endosomes (Fig. 2C) and nearly perfectly with the YFP-Rab4 early endosomes (Fig. 2D). Although we detected overall low levels of localization of mC-RhoGAP68F with the Rab7-GFP late endosomes, the proteins often localized to adjacent compartments in the apical region of the epithelium at presumptive nascent joints (Fig. 2F). The preferential localization of RhoGAP68F to the Rab4 endosomes (Fig. 2G) suggested that RhoGAP68F regulates the direct return of cargo to the cell surface from this compartment.

(D) RhoGAP68F affects the abundance, distribution and morphology of Rab4 endosomes

To determine the possible role of RhoGAP68F in endocytic control we tested whether RhoGAP68F affects the morphology, abundance and/or distribution of the Rab5, Rab4, Rab11 or Rab7 endocytic compartments. We found that expression of a moderate mC-RhoGAP68F had no effect on the morphology of the Rab5-GFP, Rab7-GFP or YFP-Rab11 endosomes and a small effect on their abundance and distribution (Supplemental Fig. 4). In contrast, expression of the moderate mC-RhoGAP68F affected both the distribution and morphology of the YFP-Rab4 endosomes (Fig. 3, Supplemental Fig. 4 G – H). In leg discs expressing YFP-Rab4 alone, the YFP-Rab4 protein accumulated at lower levels in small single vesicles (Fig. 3A). At 2 and 6h APF these vesicles accumulated at higher levels in the apical region compared to the medial region, while at 4h APF these vesicles were distributed more equally between the apical and medial regions (Fig. 3E–F). However, the expression of a moderate mC-RhoGAP68F together with YFP-Rab4 shifted the relative distribution of the YFP-Rab4 endosomes along the apicobasal axis, decreasing YFP-Rab4 accumulation in the apical region and increasing its accumulation in the medial region (Fig. 3E–F). In addition, co-expressing moderate RhoGAP68F with YFP-Rab4 led to qualitative changes in the morphology of the YFP-Rab4 endosomes - some Rab4 endosomes increased in size (compare Fig. 3B to 3A), while others formed clusters of closely apposed endosomes (compare Fig. 3C to 3A).

In leg depleted for RhoGAP68F function the YFP-Rab4 endosomes were generally more abundant at 2–6h APF, and moderately more abundant in the apical region compared to the medial region at 6h APF compared to wild type (Fig. 3D–F). Thus, while overexpression of RhoGAP68F increased the abundance of the YFP-Rab4 endosomes in the medial region compared to the apical region, depletion of RhoGAP68F increased the overall of abundance of the Rab4 endosomes and moderately increased their abundance in the apical region relative to the medial region (at 6h APF).

Taken together, these observations suggested that RhoGAP68F affects the trafficking of Rab4 endosomes and thereby the morphology and abundance of the Rab4 endosomes along the epithelium apicobasal axis.

(E) Fas3 and E-cad localize to Rab4 recycling endosomes

We hypothesized that RhoGAP68F inhibits the direct return of adhesion proteins to the cell surface in Rab4 endosomes. To identify the cargo content of the Rab4 endosomes we examined the localization of the AJs, SJs and focal adhesion proteins, E-cad, Fas3 and βPS-Integrin, respectively, relative to the Rab4 endosomes (Fig. 4). We found overall high levels of Fas3, intermediate levels of E-cad and low levels of βPS-Integrin localization in the YFP-Rab4 endosomes (Fig. 4A–B, D–E, G–H). While Fas3 and E-cad accumulated at high levels at SJs and AJs, respectively, they also accumulated at lower levels along the entire basolateral membrane domain consistent with previous reports (Langevin et al., 2005; Takeichi, 2014; Tepass and Hartenstein, 1994; Wells et al., 2013). Careful analysis of confocal sections revealed that Rab4 endosomes containing both Fas3 and E-cad were most abundant just basal to the AJs and SJs (supplemental Fig. 5B). These vesicles were clearly observed in the cytoplasm, and in apposition to the cell surface, suggesting that these

vesicles preferentially delivered Fas3 and E-cad to the cell surface in this region (Fig. 4A, D-E).

We note that while Fas3 accumulated at relatively uniform levels along the lateral membrane domain (Fig. 1B–C compare to 1 A), other SJs proteins such as Neurexin IV (Nrx-IV), ATPα and Disc large (Dlg), that seal the epithelium and participate in maintaining apicobsal polarity, accumulated in a more restricted pattern just below the AJs, and at lower levels along the lateral membrane domain (Supplemental Fig. 6). These observations support the idea that Fas3 plays special roles, distinct from the core SJs proteins, in epithelial remodeling (Wells et al., 2103).

(F) RhoGAP68F may inhibit E-cad and Fas3 return to the cell surface *in vivo*

To determine whether RhoGAP68F inhibits cargo return to the cell surface, we examined whether RhoGAP68F expression promotes Fas3 and E-cad accumulation in Rab4 endosomes. Indeed, expression of moderate mC-RhoGAP68F together with YFP-Rab4 led to the accumulation of Fas3 and E-cad in single and clusters of enlarged YFP-Rab4 endosomes consistent with this idea (Fig. 4C, F).

By inhibiting the transport of Rab4 endosomes to the cell surface RhoGAP68F could promote the accumulation of Fas3 and E-cad in cytoplasmic reservoirs or their routing for degradation in lysosomes. Consistent with this idea, both Fas3 and E-cad strongly localized to YFP-Rab7 late endosomes (supplemental Fig. 5C). Strikingly, the expression of Rab7-GFP together with moderate mC-RhoGAP68F dramatically increased the incidence of tears in the epithelium (32/43 leg analyzed) (Fig. 1H), compared to the low incidence of tears in legs expressing mC-RhoGAP68F alone (4/33; Fig. 1G), and no tears in legs expressing YFP-Rab7 alone (0/45 leg analyzed). We suspect that the simultaneous overexpression of moderate mC-RhoGAP68F and YFP-Rab7 more severely reduced the surface expression of adhesion proteins resulting in a greater incidence of epithelial tears.

(G) mC-RhoGAP68F inhibits trafficking of Fas3 in Rab4 endosomes to cell-cell contacts in S2 cells

In order to determine the role of RhoGAP68F in endocytic control, we turned to the analysis of RhoGAP68F function in S2 cells. Recapitulating the *in vivo* observations, mC-RhoGAP68F or YFP-Rab4 expressed alone localized mostly to single vesicles in S2 cells (Fig. 5A and 5B, respectively), but colocalized in clusters of enlarged vesicles when co-expressed (Fig. 5C). Expression of Fas3 alone promoted adhesion between Fas3 expressing cells (Fig. 5D–E) consistent with previous reports (Snow et al., 1989; Wells et al., 2013), and Fas3 localized preferentially to a rim between adhering cells reminiscent of E-cad localization to newly formed cell contacts *in vitro* (arrows in Fig. 5D) (Engl et al., 2014; Maitre et al., 2012). In addition, Fas3 localized to free cell surfaces, to vesicles and punctate structures in the cytoplasm. Fas3 expressed together with YFP-Rab4 and mC-RhoGAP68F, accumulated in clusters of enlarged YFP-Rab4/mC-RhoGAP68F endosomes, as well as to cell-cell contacts and free cell surfaces (Fig. 5F). Thus, the functional interactions among the three proteins observed in S2 cells recapitulated those observed *in vivo*.

To determine if RhoGAP68F affects the motion of the Rab4 endosomes, we live imaged the dynamics of YFP-Rab4 endosomes in S2 cells using spinning disc microscopy (Supplemental Fig. 7). We identified single “large vesicles” defined by their visible lumen, and single “small vesicles”, whose lumen was not visible, and separately quantified their movement. We found that in the presence of mC-RhoGAP68F, the displacement and velocity of both the small and large YFP-Rab4 vesicles were significantly reduced compared to cells expressing YFP-Rab4 alone. These observations suggest that RhoGAP68F could inhibit the trafficking of Rab4 vesicles to the cells surface in part by reducing their displacement and velocity.

To test the role of RhoGAP68F in regulation of Fas3 trafficking, we developed cell-based endocytic and recycling assays utilizing a monoclonal antibody directed against the Fas3 extracellular domain (Fig. 5G) (see material and methods for detail) (Langevin et al., 2005). To monitor endocytosis, we labeled the surface pool of Fas3 at 4°C, and then followed the movement of Fas3 from the cell surface at 25°C (for 0, 10 and 20 minutes). At time 0, Fas3 was detected in punctate structures at free cell surfaces and cell-cell contacts. After 10 minutes of chase, endocytic vesicles containing Fas3 were clearly detected in the cytoplasm, and after 20 minutes Fas3 levels decreased at free cell surfaces and increased along cell-cell contacts. To quantify Fas3 redistribution from free cell surfaces to cell contacts we measured the ratio of signal intensity at cell contacts relative to free cell surfaces at each time point. We found comparable distribution of Fas3 after 0 and 10 minutes chase in cells expressing Fas3 alone compared to cells expressing Fas3 together with RhoGAP68F. However, after 20 minutes of chase, we found a significant nearly two-fold reduction of Fas3 localization to cell-cell contacts relative to free cell surfaces in cells expressing both Fas3 and RhoGAP68F compared to cells expressing Fas3 alone (Fig. 5G). These results suggest that Rab4 endosomes deliver Fas3 from free cell surfaces to cell-cell contacts, and RhoGAP68F inhibits this process.

To test the role of RhoGAP68F in regulating the return of Fas3 from the cytoplasm to cell-cell contacts, we labeled both the cytoplasmic and surface pools of Fas3, then masked the surface pool, and followed the movement of the unmasked cytoplasmic pool to cell-cell contacts (for 0, 1, 10 and 20 minutes) (Fig. 5H). In cells expressing Fas3 alone, a fraction of the cytoplasmic pool (~35%) was trafficked to cell-cell contacts after 20 minutes of chase, compared to a smaller fraction (~16%) in cells expressing Fas3 together with mC-RhoGAP68F. These results further support the idea that RhoGAP68F inhibits the return of Fas3 to cell-cell contacts.

(H) RhoGAP68F and Fas3 interact genetically to affect epithelial organization

To test whether RhoGAP68F and Fas3 interact genetically *in vivo*, we compared the phenotypes of epithelial cells depleted for Fas3 alone, RhoGAP68F alone, and both Fas3 and RhoGAP68F (Fig. 6). We also examined the phenotypes of epithelial cells depleted for Rab4 or that overexpress RhoGAP68F. We depleted or expressed these proteins in the relatively flat epithelium of the wing imaginal disc in a stripe of Ptc-expressing cells along the anterior-posterior compartment boundary and monitored changes in epithelial bending along the future wing marging. We confirmed that the Rab4 and Fas3 RNAis depleted the

respective proteins in the epithelium of the wing disc (Supplemental Fig. 1D, Fig. 6C, E, respectively). We found that depletion of Rab4 or Fas3, or ectopic expression of RhoGAP68F, in the Ptc domain led to the bending of the epithelum (Fig. 6B, 6C, 6F, respectively). We suspect that these manipulations decrease endocytic recycling of cell adhesion proteins back to the cell surface and thereby the strength of lateral cell-cell contacts leading to epithelial bending. Strinkingly, depletion of RhoGAP68F together with Fas3 prevented the bending of the epithelium induced by depletion of Fas3 alone (Fig. 6D–E). This result suggests that RhoGAP68F depletion increased the transport of Fas3, and possibly other cell adhesion molecules such as E-cad, back to the cell surface thereby suppressing the Fas3 RNAi phenotype. This is likely to be case as we find that both Fas3 and E-cad are transported in Rab4 endosomes.

(I) Active Rab4 protein recruits the RhoGAP68F protein to the Rab4 compartment and the RhoGAP68F–Sec14 domain is sufficient for localizing to Rab4 endosomes

To understand the mechanism of RhoGAP68F recruitment to the Rab4 endocytic compartment, we examined the interaction between tagged variants of RhoGAP68F and Rab4 in S2 cells. As shown above, we found that YFP-Rab4 expressed alone localized mostly to single endocytic vesicles (Fig. 7A), while mC-RhoGAP68F and YFP-Rab4 expressed together caused enlargement and clustering of the YFP-Rab4 vesicles (Fig. 7B), similar to the effects seen *in vivo* (Fig. 3). Rab GTPases are activated by binding to GTP and are inactivated by the hydrolysis of GTP to GDP. To determine whether RhoGAP68F localization to the Rab4 compartment was dependent on the activity state of Rab4, we examined mC-RhoGAP68F localization relative to constitutively active and dominant negative Rab4 variants. Constitutively active YFP-Rab4 expressed alone localized mostly to single endosomes, which appeared larger and more abundant compared to cells expressing the wild type YFP-Rab4 protein (Fig. 7C). mC-RhoGAP68F expressed together with active YFP-Rab4 localized to the Rab4 compartment and led to further enlargement and clustering of the YFP-Rab4 endosomes, and to the formation of extensive branched tubular structures (Fig. 6D). Dominant negative YFP-Rab4 accumulated in the cytoplasm in a diffuse pattern (Fig. 7E) and RhoGAP68F accumulated in a similar diffuse pattern when co-expressed with this variant (Fig. 7F). The colocalization of RhoGAP68F with the wild type and active Rab4 variant suggested that active GTP-bound Rab4 protein recruits RhoGAP68F to Rab4 endosomes either direct or indirectly (D'Souza et al., 2014).

To test whether the RhoGAP68F N-terminal Sec 14 domain along could be targeted to the Rab4 compartment, we tagged the Sec14 domain with RFP (RFP-Sec14) and examined the distribution of the tagged RFP-Sec14 domain relative to the YFP-Rab4 endosomes. We found that the RFP-Sec14 variant localized to the Rab4 compartment both in S2 cells and *in vivo* (Fig. 7I, 7L). To determine whether the activity of the C-terminal GAP domain was required for proper targeting, we generated a GAP deficient RhoGAP68F protein by substituting a conserved Arginine at position 315 in the GAP domain to an Alanine. We found that the GAP activity of the RhoGAP68F was not required for targeting the protein to the Rab4 compartment both in S2 cells and *in vivo* (Fig. 7J, 7M). We conclude that the RhoGAP68F protein is targeted to the Rab4 compartment independent of the activity of the GAP domain, while the Sec14 domain is sufficient for localizing to the Rab4 compartment.

Both variants caused mild clustering and enlargement of Rab4 endosomes in S2 cells and *in vivo* and therefore interfered in some way with the trafficking of the Rab4 endosomes.

(J) Rab4 and RhoGAP68F can form a molecular complex

The colocalization of YFP-Rab4 and mC-RhoGAP68F both *in vivo* and in S2 cells suggested that the two proteins interact physically. To test this idea we performed co-immunoprecipitation (co-IP) assays of tagged Myc-RhoGAP68F expressed together with wild type, dominant negative or constitutively active Flag-tagged variants of Rab4 in S2 cells (Fig. 7G). We found that the Myc-RhoGAP68F protein associated with the wild type Flag-Rab4 protein. This association was stronger with the constitutively active Flag-Rab4 variant, and weaker with the dominant negative variant compared to the association with the tagged wild type protein. These results suggest that the active, membrane-associated Rab4 protein recruits RhoGAP68F to the Rab4 endosomes, where RhoGAP68F modulates the fast recycling of Rab4 endosomes back to the cell surface.

DISCUSSION

We previously showed that RhoGAP68F is expressed broadly in the epithelium of the leg imaginal disc and is upregulated at presumptive joints. Its depletion impaired the elongation of the tarsus and the invagination of the epithelium at presumptive tarsal joints and its overexpression caused a range of morphological defects (Greenberg and Hatini, 2011). In this study, we investigated the mechanisms by which RhoGAP68F affects epithelial remodeling. We found that RhoGAP68F localizes preferentially to Rab4 endosomes and functions to inhibit the direct return of Rab4 endosomes containing Fas3 and possibly E-cad to the cell surface. Functional analysis in S2 cells revealed that RhoGAP68F decreases the recycling rate and localization of Fas3, and possibly other adhesion proteins, to cell-cell contacts. In this manner, RhoGAP68F is predicted to decrease the strength of adhesive cell-cell contacts to facilitate the rearrangements of the epithelium of the leg imaginal disc during early prepupal stages. The effects of inhibition or activation of RhoGAP68F on the organization of the leg epithelium, and epistasis analysis in the wing imaginal disc support these ideas. Thus, our work connects trafficking mechanisms of an endocytic organelle engaged in trafficking adhesion proteins to the cell surface to the rearrangements of epithelial sheets during tissue morphogenesis.

Role of the RhoGAP68F–Rab4 interaction in regulation of endocytic transport

Tissue morphogenesis requires cells to change shape and contact with their neighbors. These rearrangements depend on dynamic changes in surface expression of adhesion proteins (Bryant and Stow, 2004; Wirtz-Peitz and Zallen, 2009), the stability of adhesion molecules at the cell surface (D'Souza-Schorey, 2005), and the behavior of endocytic organelles, which receive and process endocytic cargo from the cell surface (Delva and Kowalczyk, 2009; Maxfield and McGraw, 2004). Overexpression of RhoGAP68F caused clustering and enlargement of Rab4 endosomes (Fig. 3B–C) suggesting that normally the Rab4 endosomes maintain an equilibrium between fusion with incoming vesicle and transport of Rab4 vesicles back to the cell surface. Such a dynamic balance appears to control the size and distribution of Rab4 vesicles in the endocytic compartment. The clustering and enlargement

of Rab4 vesicles caused by the overexpression of RhoGAP68F and the presences of adhesion proteins in these vesicles (Fig. 4C, F) suggest that RhoGAP68F decreases the return of adhesion proteins back to the cell surface. The coincidental accumulation of Fas3 and E-cad in Rab7 late endosomes in the epithelium of the leg imaginal disc (supplemental Fig. 5C) further suggests that the inhibition of cargo return to the cell surface coordinates with the increase of cargo degradation or accumulation in a cytoplasmic reservoirs to decrease the surface expression of adhesion proteins. This coordinated changes in transport, away from the cell surface and toward late endosomes, may therefore combine to reduce the strength of adhesive cell-cell contacts to promote epithelial remodeling at early pupal stages.

Possible mechanistic role of RhoGAP68F in regulating the scission and movement of Rab4 endosomes

We have mapped a region sufficient for targeting to the Rab4 compartment to the RhoGAP68F N-terminal Sec14 domain and find that RhoGAP68F forms a complex with Rab4 using co-IP assays in S2 cells (Fig. 7). Overexpression of RhoGAP68F caused fusion and clustering of Rab4 endosomes and therefore appeared to inhibit the scission (Fig. 4) and movement of Rab4 endosomes (Supplemental Fig. 7). The budding and scission of Rab4 endosomes are dependent on the NPF WASH, the large GTPase Dynamin and microtubule (MT)-based motility factors. WASH activates the Arp2/3 complex on sorting and recycling endosomes and is required for the fission of tubules that form transport vesicles (Derivery et al., 2009; Gomez and Billadeau, 2009). The WASH-Arp2/3 complex controls actin polymerization to generate a pushing force on endosomes, while MT-based motors generate a pulling force on the membrane to promote fission from endosomes. Dynamin polymerizes around the nascent tubes, while actin polymerization could promote membrane invagination and provide tension at the vesicle neck to facilitate Dynamin-mediated scission (Roux et al., 2006). Defects in WASH or Dynamin function led to the formation of tubular structures that emanate from endosomes (Derivery et al., 2009; Gomez and Billadeau, 2009). We observed some tubular structures emanating from enlarged Rab4 endosomes (data not shown) suggesting that RhoGAP68F may inhibit WASH or dynamin activity. The primary defect induced by RhoGAP68F overexpression, however, is the clustering of Rab4 endosomes. This defect could arise from a failure to complete the process of vesicle scission, or to engage vesicles for transport on MT tracks. The enlargement of the Rab4 vesicles may be secondary to the occlusion of the Rab4 transport routes back to the cell surface. RhoGAP68F is most effective as a GAP for Rho1 (Nahm and Lee, 2011; Sanny et al., 2006) suggesting that Rho1 activates effectors for vesicle scission or movement, while RhoGAP68F antagonizes these activities of Rho1. WASH and Rho1 interact physically in *Drosophila* supporting a possible link between the two pathways (Liu et al., 2009). While WASH promotes the synthesis of branched actin filaments, Rho1 may promote the assembly of a contractile actomyosin network composed on linear actin filaments and Myosin II motors at the vesicle neck to provide the tension necessary to promote vesicle fission in parallel to WASH. Myosin II has been implicated in vesicle fission of Rab6 endosomes from the Golgi network (Miserey-Lenkei et al., 2010), but no evidence have so far have linked Myosin II to fission of Rab4 endosomes. Additional studies will be required to explore the interaction between RhoGAP68F and Rho1 and determine the mechanistic role of this interaction in endocytic scission and movement.

Developmental role of RhoGAP68F in control of cell adhesion and tissue morphogenesis

We find that Fas3 and E-cad localize to Rab4 endosomes (Fig. 4 and Supplemental Fig. 5) suggesting that these adhesion proteins are returned back to the cell surface from sorting endosomes. The presence of a persistent pathway for the direct return of adhesion proteins back to the cell surface provides the capacity for epithelial cells to rapidly fine tune their adhesion and morphology during tissue morphogenesis in response to intrinsic and extrinsic biochemical and mechanical inputs. Our data suggest that the regulation of this persistent pathway allows epithelial cells to modulate cell adhesion dynamically during development.

We find that Fas3 levels are modulated both at the plane and along the apicobsal axis of the leg epithelium (Fig. 1A–C). At the plane of the epithelium, Fas3 levels are higher proximal to the presumptive joints and lower within and distal to the joints. Along the lateral membrane domain, Fas3 accumulates uniformly at early prepupal stages, while at later stages it becomes restricted to the subapical region just below the AJs. Modulation of both the planar and apicobasal distributions of Fas3 may affect the strength of lateral adhesive contracts and the mechanical properties of the epithelium. Modulation of the surface expression of E-cad at AJs has been shown to influence the shape of embryos, tissues and organs (Classen et al., 2005; Hayashi and Carthew, 2004; Levayer et al., 2011; Mateus et al., 2011; Shaye et al., 2008; Tanaka-Matakatsu et al., 1996; Uemura et al., 1996; Warrington et al., 2013). More recently, mechanisms affecting the abundance and distribution of SJs proteins have also been implicated in the regulation of cell shape changes and tissue level morphogenesis in several tissues. In the follicular epithelium, a decrease in surface expression of Fasciclin 2 (Fas2) was linked to the shortening of lateral cell contacts from cuboidal to squamous (Szafranski and Goode, 2004). The Sterile 20 protein kinase Tao controls this transition by promoting Fas2 endocytosis from the lateral cell surface (Gomez et al., 2012). In the tubular epithelium of the hindgut, the asymmetric expression of Fas3 to one sector of the hindgut and the accumulation of Fas3 along the lateral membrane domain, have been shown to account for hindgut curvature (Wells et al., 2103). Similarly, the pattern of Fas3 expression across leg segments and the modulation of Fas3 distribution along the lateral membrane domain may reinforce the relatively flat morphology of the leg epithelium at early stages, and the pattern of folds and bulges of the epithelium at presumptive segment and joints, respectively, at later stages. We note that neither broad expression of Fas3 nor loss of *fas3* function in large clones generated in a Minute background impaired leg development (data not shown). In contrast, ectopic expression or depletion of RhoGAP68F elicited strong phenotypes suggesting that RhoGAP68F regulates the trafficking of additional adhesion proteins to lateral cell adhesion zones including E-cad. This is likely to be the case given that RhoGAP68F affects the behavior of an entire endocytic organelle that preferentially recycles cargo to the lateral cell surface.

A revised model for epithelial morphogenesis of the leg imaginal disc

During development, the epithelium of the leg imaginal disc changes its morphology from pseudostratified to simple (Fig. 1A–C). We hypothesize that the localization of Fas3, and possibly other adhesion proteins, to the lateral membrane domain supports the pseudstratified organization of the epithelium at larval stages. During this period, Fas3 and E-cad are endocytosed and recycled back to the plasma membrane. Disc elongation is

enabled by signals that act globally at the onset of metamorphic development to loosen the apical extracellular matrix and increase the internal hydrostatic pressure to expand the tubular epithelium of the leg disc (Fristrom et al., 1978; von Kalm et al., 1995). These global events somehow enable progression of cellular events that narrow and elongate the leg disc. These processes coincide with and possibly trigger the endocytic internalization of adhesion proteins. Expression analysis revealed that RhoGAP68F levels peak at the onset of prepupal development (modENCODE: The Drosophila Transcriptome (http://www.modencode.org/Celniker.shtml)) suggesting that RhoGAP68F upregulation could be used as a developmental mechanism to downregulate the transport of adhesion proteins back to the cell surface, and thereby increase cargo transport toward late endosomes. The resulting decrease in surface expression of adhesion molecules and the strength of adhesive cell-cell contacts could enable epithelial cells to remodel more freely their shape and cell-cell contact to facilitate the narrowing and elongation of the leg PD axis. The upregulation of *RhoGAP68F* expression at presumptive joints (Greenberg and Hatini, 2011) suggests that it is preferentially required in this region to accelerate membrane and junctional remodeling required for apical constriction. Consistent with this idea, ectopic expression of RhoGAP68F in the Ptc domain of the wing imaginal disc led to the invagination of the epithelium in this region (Fig. 6F). Likewise, depletion of Rab4 or Fas3 in the Ptc domain led to similar phenotypes (Fig. 6B and C, respectively). However, epithelial invagination was suppressed by depletion of RhoGAP68F together with Fas3 (Fig. 6E) providing evidence that RhoGAP68F promotes epithelial invagination by inhibiting Fas3 return to the cell surface in Rab4 endosomes. Broad expression of a moderately strong RhoGAP68F led to tears of the epithelium preferentially proximal to presumptive joints a phenotype that was enhanced by co-expression of Rab7-GFP (Fig 1G and H, respectively). Broadly inhibiting the return of adhesion receptors to the cell surface may have weakened adhesive interactions between cells, and thereby compromised the integrity of the tension-bearing parts of the tissue leading to the detachments of cell-cell contacts in these regions. Overall, these results support a model whereby a decrease in lateral adhesions enables the epithelium to buckle at presumptive joints, whereas a moderate and general decrease in adhesion facilitates the global rearrangements of cell shape and cell contacts mediating elongation. These differential changes in adhesion are regulated by the broad upregulation of RhoGAP68F in the epithelium of the leg imaginal disc and the preferential upregulation of RhoGAP68F at presumptive joints.

Concluding remarks

The results presented in this work uncovered for the first time a role for Rab4 endosomes in trafficking E-cad and Fas3 to the cell surface in epithelial cells, and a role for RhoGAP68F in modulating the return of Rab4 endosomes back to the cell surface. The anomalies in planar and apicobasal rearrangements of the epithelium of legs depleted for RhoGAP68F or that overexpress RhoGAP68F and the associated trafficking anomalies suggest important roles for fast endocytic recycling of junctional proteins from early endosomes during epithelial tissue morphogenesis. The work shed light on an aspect of epithelial tissue morphogenesis that is relatively less well investigated and new avenues for further understanding of the regulation of trafficking pathways of cell adhesion proteins involved in epithelial morphogenesis.

MATERIAL & METHODS

Fly lines

The following fly lines were generated in this study: *UAS-mCherry-RhoGAP68F* (strong #159, moderate #171, and weak #157), *UAS-RFP-RhoGAP68F*, *UAS-RFP-RhoGAP68F (R315A)*, *UAS-RFP-RhoGAP68F–Sec14*, *UAS-Fas3*. Other fly lines used include: *UAS-YFP-Rab4* and *UAS-YFP-Rab11*, (Bloomington Stock Center), *UAS-Rab7-GFP* (Entchev et al., 2000), *UAS-Rab5-GFP* (Wucherpfennig et al., 2003), *UAS-RhoGAP68FRNAi* (VDRC ID34250, ID107775 & TRiPJF01605 strong, ID34249 weak insertions), *UAS-Fas3RNAi* (VDRC ID939>ID940>ID3091>ID26357), *UAS-Rab4RNAi* (VDRC ID24672, ID106651 strong insertions), *Dll-GAL4^{md23}*, *Ptc-GAL4$^{559.1}$; UAS-CD8-RFP* and *y w hsFLP; Ubi-RFP FRT40A* (Bloomington Stock Center), *fas3^{A142} 40AFRT* (DGRC-Kyoto), y w *hsFLP; Ubi-GFP M(2)24F[1] FRT40A* (gift of E. Moreno).

Molecular Biology

The *RhoGAP68F* open reading frame (ORF) was amplified from cDNA clone LD02491 and the PCR product was fused in frame with corresponding tags in pCS2 2X–Flag (gift from P. Klein) and pCS2-mCherry (gift from R. Tsien). Three glycine codons were included in the 5’ PCR primer to separate the tags from the RhoGAP68F protein. Tagged ORFs were then cloned into the pUAST transformation vectors using restriction enzymes and transgenic flies carrying these transgenes were established by standard method by Genetic Services Inc. All other constructs were generated by the Gateway technology (Walhout et al. 2000) using the *Drosophila* Gateway Vector Collection (gift of T. Murphy). The 477 amino acids long RhoGAP68F protein is composed of an N-terminal Sec14 domain spanning amino acids 94–241 and a C-terminal GAP domain spanning amino acids 290–461. The intact RhoGAP68F ORF was used to generate *pActin-RFP-RhoGAP68F* and *pActin-Myc-RhoGAP68F*. Site-directed mutagenesis was performed to inactivate the GAP domain by substituting the Arginine at position to 315 to Alanine to generate *pActin-RFP-RhoGAP68F (R315A)* and *pActin-Myc-RhoGAP68F (R315A)* GAP-deficient variants. The Sec14-only variant was generated by amplification of a region spanning amino acids 94–241 to generate *pActin-RFP-GAP68F–Sec 14* and *pActin-Myc-GAP68-Sec14*. *pUASp-YFP-Rab4* wild type, constitutively active and dominant negative variants have been previously described (Walhout, 2000). The ORFs of these variants were amplified from plasmid DNA (gift from M. Scott) and used to generate *pActin-Flag-Rab4* and mutant variants. The ORF of Fas3 was amplified from cDNA clone RE66907 and used to generate *pUASp-Fas3* and *pActin-Fas3* variants.

Trafficking assays

Fluid phase endocytosis—Dissected discs were incubated with 5 g/ml Cascade Blue conjugated dextran (Molecular Probes) in M3 insect medium at 25°C for 10 min (pulse), followed by five washes in ice-cold M3 medium for 2 min each. Discs were chased for 20 min or for 1 hour in M3 medium at 25°C to visualize early or late endosomes, respectively (Entchev et al., 2000). Following the chase, the discs were fixed in 4% formaldehyde for 35 minutes at 25°C and processed for analysis.

Endocytic Assay—To test the effect of RhoGAP68F on Fas3 endocytosis, S2 cells were transfected with 2μg of *pActin-Fas3* alone and separately with 2μg *pActin-Fas*3 together with 2μg *pActin-RFP-RhoGAP68F* in 6 cm dishes at 50% confluence. 2 days after transfection, cells were plated on 22 mm coverslips, washed with ice cold PBS and incubated with 100μl of mouse anti-Fas3 (1:50 dilution in S2 culture medium) for 20 min at 4°C to label the surface pool of Fas3. The cells were then washed twice with ice cold PBS. One set of samples was fixed with 2% formaldehyde and stained (with Cy5-conjugated anti-mouse secondary antibodies) to measure Fas3 levels at the cell surface before the chase (time 0). The remaining samples were chased for 1, 10 and 20 min at 25°C.

Recycling Assay—To test whether RhoGAP68F affects the return of Fas3 to the cell surface, S2 cells were transfected with 1μg *pActin-Fas3* alone and separately with 1μg *pActin-Fas3* together with 1μg *pActin-RFP-RhoGAP68F* in 6 cm dishes at 50% confluence. Two days after transfections the cells were collected and incubated for 10 min on a rocking platforms to allow the cells to partially reaggregate. The cells were then allowed to adhere for 40 min onto 22 mm coverslips. Adherent cells were washed once with PBS, and incubated with 100μl of mouse anti-Fas3 in S2 culture medium for 1h at 25C°. One set of samples was fixed and stained to label the surface pool of Fas3. Remaining samples were incubated at 4°C for 10 min to stop endocytic trafficking. The coverslips were washed in PBS and incubated with 100μl of unconjugated goat anti-mouse IgG (1:50 in PBS; Jackson ImmunoResearch) for 30 min to quench the surface pool of Fas3. A second set of samples was fixed after this step and stained with Cy5-conjugated anti-mouse secondary antibodies to measure quenching efficiency, which typically approached 80% (20% of original signal remaining). To follow the recycling of Fas3 back to the surface, the samples were then chased for 1, 10 and 20 min in S2 culture medium at 25°C.

Following the chase, discs were fixed to terminate endocytic trafficking and processed for analysis by immunofluoresnce. The fixed cells were stained with mouse anti-Fas3 antibodies and Cy5-conjugated 2° anti-mouse antibodies. All samples were scanned under the same setting using confocal microscopy and mean signal intensity along cell contacts and free cell surfaces were measured in selected ROis. For endocytic assays, the Fas3 mean gray pixel intensity was measured in a single plane where the fluorescent signal at cell contacts was the highest. For recycling assays, the Fas3 mean gray pixel intensity was measured at cell contacts only. ROi were demarcated using the free-hand tool in Fiji (NIH) in 10 pixel wide regions.

Analysis of Rab4 vesicle dynamic—Vesicle dynamics were monitored by time lapse spinning disc microscopy (Perkin Elmer, Ultraview). Vesicles were manually tracked in Volocity (Perkin Elmer) to measure their velocity and displacement.

Statistics

Statistical analyses were preformed using Microsoft Excel. P-values were calculated using a two-tailed unpaired *t*-test.

Immunoprecipitation assays

To analyze the interaction of Myc-RhoGAP68F with Flag-Rab4 or activated or dominant negative mutant variants, S2 cells at 50% confluence were transfected using calcium phosphate in 6-cm dishes with 1μg of *pActin-Myc-GAP68F* and 1μg of *pActin-Flag-Rab4* and corresponding mutant variants. Immunoprecipitation assays were performed as previously described (Hatini et al., 2005, Green et al., 2002) using anti-Flag antibodies for Rab4 (M2; Sigma) at 1:40 dilution, followed by immunoblotting with rabbit anti-Myc (A-14; Santa Cruz) at 1:1000 dilution. The amounts of the immunoprecipitated Flag-Rab4 were used to normalize for variations in transfection efficiency.

Antibodies and immunofluorescence of leg imaginal discs

Larvae of desired genotypes were transferred to 30°C from 25°C 48h prior to dissection. At the day of dissection, desired white prepupa (0h APF) were selected, transferred to a glass slide and aged for 2, 4 or 6 hours (2, 4 and 6 hours APF) at 25°C. Discs were then dissected and processed for immunofluoresnce using standard protocols. The following antibodies were used: rat anti-E- cadherin (1:100, DCAD2, DSHB), mouse anti-Fas3 (1:50; 7G10, DSHB). Rabbit anti-Rab4 and rabbit anti-RhoGAP68F were raised using standard protocol in this study by ProSci Incorporated against unique peptide sequences spanning amino acid 15–35 (AINPIVDNSDEPQPSLSDLHD) and 80–100 (EDDFEDQLREQSENFQTPRNK) for RhoGAP68F, and 118–135 (LVGNKKDLEEARDVTFLE) and 189–208 (YGGAALRNLQTRQRSINKPD) for Rab4. The RhoGAP68F antibody failed to detect RhoGAP68F protein in imaginal discs. the Rabbit anti-Rab4 was used at 1:1000. Secondary antibodies conjugated to the Cy2, Cy3 and Cy5 fluorophores (Jackson ImmunoResearch) were used at 1:100, 1:150 and 1:50, respectively. Stained discs were scanned using a Zeiss LSM510 confocal microscope in multi-tracking mode. Images were assembled and adjusted using Adobe Photoshop CS3.

Supplementary Material

Refer to Web version on PubMed Central for supplementary material.

Acknowledgements

We thank the Bloomington Stock Center, the Vienna Drosophila Research Center (VDRC), the DGRC-Kyoto, and the TRiP at Harvard Medical School for providing transgenic fly stocks, the DGRC-Indiana for providing cell lines and cDNAs, and the Developmental Studies Hybridoma Bank for providing monoclonal antibodies. We thank Steven Del Signore and members of the Hatini lab for discussions. This work was supported by a grant from the NIH to V.H. (R01GM06806).

REFERENCES

Bankaitis VA, Mousley CJ, Schaaf G. The Sec14 superfamily and mechanisms for crosstalk between lipid metabolism and lipid signaling. Trends Biochem Sci. 2010; 35:150–160. [PubMed: 19926291]

Bertet C, Sulak L, Lecuit T. Myosin-dependent junction remodelling controls planar cell intercalation and axis elongation. Nature. 2004; 429:667–671. [PubMed: 15190355]

Bilder D, Li M, Perrimon N. Cooperative regulation of cell polarity and growth by Drosophila tumor suppressors. Science. 2000; 289:113–116. [PubMed: 10884224]

Blankenship JT, Backovic ST, Sanny JS, Weitz O, Zallen JA. Multicellular rosette formation links planar cell polarity to tissue morphogenesis. Dev Cell. 2006; 11:459–470. [PubMed: 17011486]

Bryant DM, Stow JL. The ins and outs of E-cadherin trafficking. Trends Cell Biol. 2004; 14:427–434. [PubMed: 15308209]

Bucci C, Parton RG, Mather IH, Stunnenberg H, Simons K, Hoflack B, Zerial M. The small GTPase rab5 functions as a regulatory factor in the early endocytic pathway. Cell. 1992; 70:715–728. [PubMed: 1516130]

Bucci C, Thomsen P, Nicoziani P, McCarthy J, van Deurs B. Rab7: a key to lysosome biogenesis. Mol Biol Cell. 2000; 11:467–480. [PubMed: 10679007]

Cavey M, Rauzi M, Lenne PF, Lecuit T. A two-tiered mechanism for stabilization and immobilization of E-cadherin. Nature. 2008; 453:751–756. [PubMed: 18480755]

Chen W, Feng Y, Chen D, Wandinger-Ness A. Rab11 is required for trans-golgi network-to-plasma membrane transport and a preferential target for GDP dissociation inhibitor. Mol Biol Cell. 1998; 9:3241–3257. [PubMed: 9802909]

Classen AK, Anderson KI, Marois E, Eaton S. Hexagonal packing of Drosophila wing epithelial cells by the planar cell polarity pathway. Dev Cell. 2005; 9:805–817. [PubMed: 16326392]

Condic ML, Fristrom D, Fristrom JW. Apical cell shape changes during Drosophila imaginal leg disc elongation: a novel morphogenetic mechanism. Development. 1991; 111:23–33. [PubMed: 2015798]

Curwin AJ, Fairn GD, McMaster CR. Phospholipid transfer protein Sec14 is required for trafficking from endosomes and regulates distinct trans-Golgi export pathways. J Biol Chem. 2009; 284:7364–7375. [PubMed: 19129178]

D'Souza RS, Semus R, Billings EA, Meyer CB, Conger K, Casanova JE. Rab4 Orchestrates a Small GTPase Cascade for Recruitment of Adaptor Proteins to Early Endosomes. Curr Biol. 2014; 24:1187–1198. [PubMed: 24835460]

D'Souza-Schorey. Disassembling adherence junctions: breaking up is hard to do. Trends Cell Biol. 2005; 15:19–26. [PubMed: 15653074]

Delva E, Kowalczyk AP. Regulation of cadherin trafficking. Traffic. 2009; 10:259–267. [PubMed: 19055694]

Derivery E, Sousa C, Gautier JJ, Lombard B, Loew D, Gautreau A. The Arp2/3 activator WASH controls the fission of endosomes through a large multiprotein complex. Dev Cell. 2009; 17:712–723. [PubMed: 19922875]

Dietzl G, Chen D, Schnorrer F, Su KC, Barinova Y, Fellner M, Gasser B, Kinsey K, Oppel S, Scheiblauer S, Couto A, Marra V, Keleman K, Dickson BJ. A genome-wide transgenic RNAi library for conditional gene inactivation in Drosophila. Nature. 2007; 448:151–156. [PubMed: 17625558]

Engl W, Arasi B, Yap LL, Thiery JP, Viasnoff V. Actin dynamics modulate mechanosensitive immobilization of E-cadherin at adherens junctions. Nat Cell Biol. 2014; 16:587–594. [PubMed: 24859003]

Entchev EV, Schwabedissen A, Gonzalez-Gaitan M. Gradient formation of the TGF-beta homolog Dpp. Cell. 2000; 103:981–991. [PubMed: 11136982]

Fricke R, Gohl C, Dharmalingam E, Grevelhorster A, Zahedi B, Harden N, Kessels M, Qualmann B, Bogdan S. Drosophila Cip4/Toca-1 integrates membrane trafficking and actin dynamics through WASP and SCAR/WAVE. Curr Biol. 2009; 19:1429–1437. [PubMed: 19716703]

Fristrom D, Chihara C. The mechanism of evagination of imaginal discs of Drosophila melanogaster. V. Evagination of disc fragments Dev Biol. 1978; 2:564–570.

Genova JL, Fehon RG. Neuroglian, Gliotactin, and the Na+/K+ ATPase are essential for septate junction function in Drosophila. J Cell Biol. 2003; 161:979–989. [PubMed: 12782686]

Georgiou M, Marinari E, Burden J, Baum B. Cdc42, Par6, and aPKC regulate Arp2/3-mediated endocytosis to control local adherens junction stability. Curr Biol. 2008; 18:1631–1638. [PubMed: 18976918]

Gomez JM, Wang Y, Riechmann V. Tao controls epithelial morphogenesis by promoting Fasciclin 2 endocytosis. J Cell Biol. 2012; 199:1131–1143. [PubMed: 23266957]

Gomez TS, Billadeau DD. A FAM21-containing WASH complex regulates retromer-dependent sorting. Dev Cell. 2009; 17:699–711. [PubMed: 19922874]

Green RB, Hatini V, Johansen KA, Liu XJ, Lengyel JA. Drumstick is a zinc finger protein that antagonizes Lines to control patterning and morphogenesis of the Drosophila hindgut. Development. 2002; 129:3645–3656. [PubMed: 12117814]

Greenberg L, Hatini V. Systematic expression and loss-of-function analysis defines spatially restricted requirements for Drosophila RhoGEFs and RhoGAPs in leg morphogenesis. Mech Dev. 2011; 128:5–17. [PubMed: 20851182]

Guillot C, Lecuit T. Mechanics of epithelial tissue homeostasis and morphogenesis. Science. 2013; 340:1185–1189. [PubMed: 23744939]

Gumbiner BM. Regulation of cadherin-mediated adhesion in morphogenesis. Nat Rev Mol Cell Biol. 2005; 6:622–634. [PubMed: 16025097]

Harris KP, Tepass U. Cdc42 and Par proteins stabilize dynamic adherens junctions in the Drosophila neuroectoderm through regulation of apical endocytosis. J Cell Biol. 2008; 183:1129–1143. [PubMed: 19064670]

Hatini V, Green RB, Lengyel JA, Bray SJ, S Dinardo S. The Drumstick/Lines/Bowl regulatory pathway links antagonistic Hedgehog and Wingless signaling inputs to epidermal cell differentiation. Genes Dev. 2005; 19:709–718. [PubMed: 15769943]

Hayashi T, Carthew RW. Surface mechanics mediate pattern formation in the developing retina. Nature. 2004; 431:647–652. [PubMed: 15470418]

Heisenberg CP, Bellaiche Y. Forces in tissue morphogenesis and patterning. Cell. 2013; 153:948–962. [PubMed: 23706734]

Langevin J, Morgan MJ, Sibarita JB, Aresta S, Murthy M, Schwarz T, Camonis J, Bellaiche Y. Drosophila exocyst components Sec5, Sec6, and Sec15 regulate DE-Cadherin trafficking from recycling endosomes to the plasma membrane. Dev Cell. 2005; 9:365–376. [PubMed: 16224820]

Laprise P, Lau KM, Harris KP, Silva-Gagliardi NF, Paul SM, Beronja S, Beitel GJ, McGlade CJ, Tepass U. Yurt, Coracle, Neurexin IV and the Na(+),K(+)-ATPase form a novel group of epithelial polarity proteins. Nature. 2009; 459:1141–1145. [PubMed: 19553998]

Lee JY, Harland RM. Endocytosis is required for efficient apical constriction during Xenopus gastrulation. Curr Biol. 2010; 20:253–258. [PubMed: 20096583]

Leibfried A, Fricke R, Morgan MJ, Bogdan S, Bellaiche Y. Drosophila Cip4 and WASp define a branch of the Cdc42-Par6-aPKC pathway regulating E-cadherin endocytosis. Curr Biol. 2008; 18:1639–1648. [PubMed: 18976911]

Levayer R, Lecuit T. Oscillation and polarity of E-cadherin asymmetries control actomyosin flow patterns during morphogenesis. Dev Cell. 2013; 26:162–175. [PubMed: 23871590]

Levayer R, Pelissier-Monier A, Lecuit T. Spatial regulation of Dia and Myosin-II by RhoGEF2 controls initiation of E-cadherin endocytosis during epithelial morphogenesis. Nat Cell Biol. 2011; 13:529–540. [PubMed: 21516109]

Liu R, Abreu-Blanco MT, Barry KC, Linardopoulou EV, Osborn GE, Parkhurst SM. Wash functions downstream of Rho and links linear and branched actin nucleation factors. Development. 2009; 136:2849–2860. [PubMed: 19633175]

Maitre JL, Berthoumieux H, Krens SF, Salbreux G, Julicher F, Paluch E, Heisenberg CP. Adhesion functions in cell sorting by mechanically coupling the cortices of adhering cells. Science. 2012; 338:253–256. [PubMed: 22923438]

Martin AC, Kaschube M, Wieschaus EF. Pulsed contractions of an actin-myosin network drive apical constriction. Nature. 2009; 457:495–499. [PubMed: 19029882]

Mateus AM, Gorfinkiel N, Schamberg S, Martinez Arias A. Endocytic and recycling endosomes modulate cell shape changes and tissue behaviour during morphogenesis in Drosophila. PLoS One. 2011; 6:e18729. [PubMed: 21533196]

Maxfield FR, McGraw TE. Endocytic recycling. Nat Rev Mol Cell Biol. 2004; 5:121–132. [PubMed: 15040445]

Mirth C, Akam M. Joint development in the Drosophila leg: cell movements and cell populations. Dev Biol. 2002; 246:391–406. [PubMed: 12051824]

Miserey-Lenkei S, Chalancon G, Bardin S, Formstecher E, Goud B, Echard A. Rab and actomyosin-dependent fission of transport vesicles at the Golgi complex. Nat Cell Biol. 2010; 12:645–654. [PubMed: 20562865]

Nahm M, Lee S. Characterization of the Rho GTPase-Activating Protein RhoGAP68F. Exp Neurobiol. 2011; 20:29–34. [PubMed: 22110359]

Ni JQ, Liu LP, Binari R, Hardy R, Shim HS, Cavallaro A, Booker M, Pfeiffer BD, Markstein M, Wang H, Villalta C, Laverty TR, Perkins LA, Perrimon N. A Drosophila resource of transgenic RNAi lines for neurogenetics. Genetics. 2009; 182:1089–1100. [PubMed: 19487563]

Oda H, Uemura T, Harada Y, Iwai Y, Takeichi M. A Drosophila homolog of cadherin associated with armadillo and essential for embryonic cell-cell adhesion. Dev Biol. 1994; 165:716–726. [PubMed: 7958432]

Oshima K, Fehon RG. Analysis of protein dynamics within the septate junction reveals a highly stable core protein complex that does not include the basolateral polarity protein Discs large. J Cell Sci. 2011; 124:2861–2871. [PubMed: 21807950]

Press B, Feng Y, Hoflack B, Wandinger-Ness A. Mutant Rab7 causes the accumulation of cathepsin D and cation-independent mannose 6-phosphate receptor in an early endocytic compartment. J Cell Biol. 1998; 140:1075–1089. [PubMed: 9490721]

Ren M, Xu G, Zeng J, De Lemos-Chiarandini C, Adesnik M, Sabatini DD. Hydrolysis of GTP on rab1 1 is required for the direct delivery of transferrin from the pericentriolar recycling compartment to the cell surface but not from sorting endosomes. Proc Natl Acad Sci U S A. 1998; 95:6187–6192. [PubMed: 9600939]

Ridley AJ. Rho GTPases and actin dynamics in membrane protrusions and vesicle trafficking. Trends Cell Biol. 2006; 16:522–529. [PubMed: 16949823]

Roux A, Uyhazi K, Frost A, De Camilli P. GTP-dependent twisting of dynamin implicates constriction and tension in membrane fission. Nature. 2006; 441:528–531. [PubMed: 16648839]

Saito K, Tautz L, Mustelin T. The lipid-binding SEC14 domain. Biochim Biophys Acta. 2007; 1771:719–726. [PubMed: 17428729]

Sanny J, Chui V, Langmann C, Pereira C, Zahedi B, Harden N. Drosophila RhoGAP68F is a putative GTPase activating protein for RhoA participating in gastrulation. Dev Genes Evol. 2006; 216:543–550. [PubMed: 16609869]

Schaaf G, Ortlund EA, Tyeryar KR, Mousley CJ, Ile KE, Garrett TA, Ren J, Woolls MJ, Raetz CR, Redinbo MR, Bankaitis VA. Functional anatomy of phospholipid binding and regulation of phosphoinositide homeostasis by proteins of the sec14 superfamily. Mol Cell. 2008; 29:191–206. [PubMed: 18243114]

Shaye DD, Casanova J, Llimargas M. Modulation of intracellular trafficking regulates cell intercalation in the Drosophila trachea. Nat Cell Biol. 2008; 10:964–970. [PubMed: 18641639]

Sirokmany G, Szidonya L, Kaldi K, Gaborik Z, Ligeti E, Geiszt M. Sec14 homology domain targets p50RhoGAP to endosomes and provides a link between Rab and Rho GTPases. J Biol Chem. 2006; 281:6096–6105. [PubMed: 16380373]

Snow PM, Bieber AJ, Goodman CS. Fasciclin III: a novel homophilic adhesion molecule in Drosophila. Cell. 1989; 59:313–323. [PubMed: 2509076]

Stenmark H. Rab GTPases as coordinators of vesicle traffic. Nat Rev Mol Cell Biol. 2009; 10:513–525. [PubMed: 19603039]

Sun YJ, Nishikawa K, Yuda H, Wang YL, Osaka H, Fukazawa N, Naito A, Kudo Y, Wada K, Aoki S. Solo/Trio8, a membrane-associated short isoform of Trio, modulates endosome dynamics and neurite elongation. Mol Cell Biol. 2006; 26:6923–6935. [PubMed: 16943433]

Szafranski P, Goode S. A Fasciclin 2 morphogenetic switch organizes epithelial cell cluster polarity and motility. Development. 2004; 131:2023–2036. [PubMed: 15056617]

Tajiri R, Misaki K, Yonemura S, Hayashi S. Joint morphology in the insect leg: evolutionary history inferred from Notch loss-of-function phenotypes in Drosophila. Development. 2011; 138:4621–4626. [PubMed: 21989911]

Takeichi M. Dynamic contacts: rearranging adherens junctions to drive epithelial remodelling. Nat Rev Mol Cell Biol. 2014; 15:397–410. [PubMed: 24824068]

Tanaka-Matakatsu M, Uemura T, Oda H, Takeichi M, Hayashi S. Cadherin-mediated cell adhesion and cell motility in Drosophila trachea regulated by the transcription factor Escargot. Development. 1996; 122:3697–3705. [PubMed: 9012491]

Taylor J, Adler PN. Cell rearrangement and cell division during the tissue level morphogenesis of evaginating Drosophila imaginal discs. Dev Biol. 2008; 313:739–751. [PubMed: 18082159]

Tepass U, Gruszynski-DeFeo E, Haag TA, Omatyar L, Torok T, Hartenstein V. shotgun encodes Drosophila E-cadherin and is preferentially required during cell rearrangement in the neurectoderm and other morphogenetically active epithelia. Genes Dev. 1996; 10:672–685. [PubMed: 8598295]

Tepass U, Hartenstein V. The development of cellular junctions in the Drosophila embryo. Dev Biol. 1994; 161:563–596. [PubMed: 8314002]

Uemura T, Oda H, Kraut R, Hayashi S, Kotaoka Y, Takeichi M. Zygotic Drosophila E-cadherin expression is required for processes of dynamic epithelial cell rearrangement in the Drosophila embryo. Genes Dev. 1996; 10:659–671. [PubMed: 8598294]

van der Sluijs P, Hull M, Webster P, Male P, Goud B, Mellman I. The small GTP-binding protein rab4 controls an early sorting event on the endocytic pathway. Cell. 1992; 70:729–740. [PubMed: 1516131]

Vitelli R, Santillo M, Lattero D, Chiariello M, Bifulco M, Bruni CB, Bucci C. Role of the small GTPase Rab7 in the late endocytic pathway. J Biol Chem. 1997; 272:4391–4397. [PubMed: 9020161]

von Kalm L, Fristrom D, Fristrom J. The making of a fly leg: a model for epithelial morphogenesis. Bioessays. 1995; 17:693–702. [PubMed: 7661850]

Walhout AJ, Temple GF, Brasch MA, Hartley JL, Lorson MA, van den Heuvel S, Vidal M. GATEWAY recombinational cloning: application to the cloning of large numbers of open reading frames or ORFeomes. Methods Enzymol. 2000; 328:575–592. [PubMed: 11075367]

Warrington SJ, Strutt H, Strutt D. The Frizzled-dependent planar polarity pathway locally promotes E-cadherin turnover via recruitment of RhoGEF2. Development. 2013; 140:1045–1054. [PubMed: 23364328]

Wells RE, Barry JD, Warrington SJ, Cuhlmann S, Evans P, Huber W, Strutt D, Zeidler MP. Control of tissue morphology by Fasciclin III-mediated intercellular adhesion. Development. 2013; 140:3858–3868. [PubMed: 23946443]

Wirtz-Peitz F, Zallen JA. Junctional trafficking and epithelial morphogenesis. Curr Opin Genet Dev. 2009; 19:350–356. [PubMed: 19559596]

Wucherpfennig T, Wilsch-Brauninger M, Gonzalez-Gaitan M. Role of Drosophila Rab5 during endosomal trafficking at the synapse and evoked neurotransmitter release. J Cell Biol. 2003; 161:609–624. [PubMed: 12743108]

Yap AS, Crampton MS, Hardin J. Making and breaking contacts: the cellular biology of cadherin regulation. Curr Opin Cell Biol. 2007; 19:508–514. [PubMed: 17935963]

Zhang J, Schulze KL, Hiesinger PR, Suyama K, Wang S, Fish M, Acar M, Hoskins RA, Bellen HJ, Scott MP. Thirty-one flavors of Drosophila rab proteins. Genetics. 2007; 176:1307–1322. [PubMed: 17409086]

HIGHLIGHTS

- Rab4 endosomes traffic Fasciclin 3 and E-cadherin back to the cell surface
- Rab4 binds and recruits RhoGAP68F to the Rab4 compartment
- RhoGAP68F inhibits endocytic trafficking of Fas3 to cell contacts in S2 cells
- Overexpression of RhoGAP68F promotes enlargement and clustering of Rab4 endosomes
- Overexpression of RhoGAP68F can compromise epithelial integrity

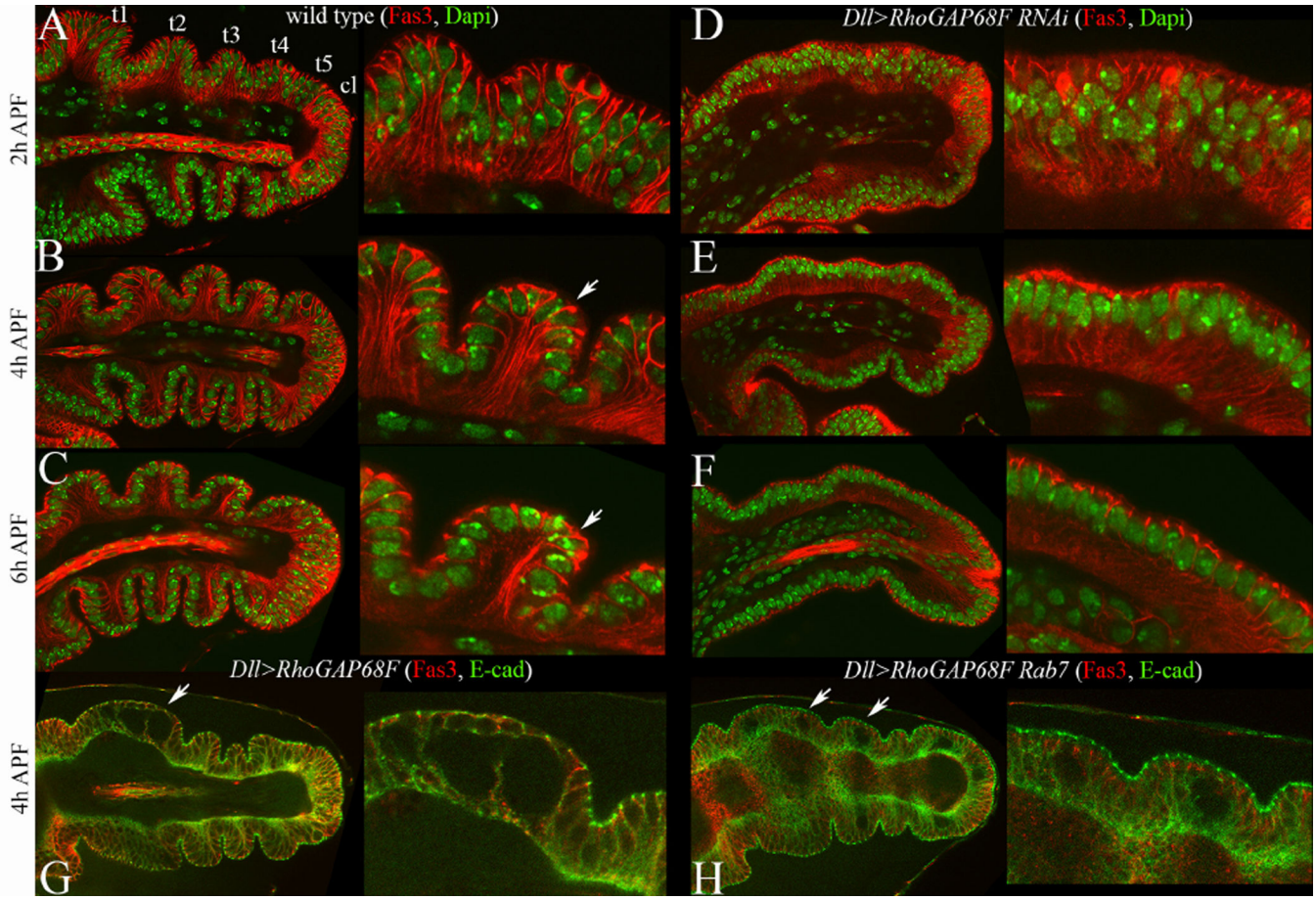

Figure 1.

Tarsal morphogenesis at early prepupal stages was impaired by depletion or overexpression of RhoGAP68F. Apicobasal sections along the proximodistal (PD) axis of the tarsal region of (A–C) wild type and (D–F) *Dll>RhoGAP68F RNAi*, stained with Fas3 (red) and Dapi (Green), (G) *Dll>RhoGAP68F* and (H) and *Dll>RhoGAP68F UAS-Rab7-GFP* stained for Fas3 (red) and E-cad (green; Rab7-GFP pattern not shown, E-cad fluorescence pseudocolored green). (A–C) During 2–6h APF the tarsal region progressively narrows and elongates. This coincides with the progressive remodeling of the epithelium from a mostly pseudostratified at 2h to simple at 4 to 6h APF. Zooms in insets show the progressive invagination of the epithelium between tarsal segment 4 (t4) and 5 (t5). At 2h APF, Fas3 localizes along the entire lateral surface of epithelial cells. At later stages, Fas3 accumulates at higher levels proximal to nascent joints where it highlights the entire lateral surface (arrows in insets in B-C). Within and distal to presumptive joints, Fas3 is lost from the lateral cell surface and becomes restricted to the subapical region. (D–F) In leg depleted for RhoGAP68F, the invagination of the epithelium at presumptive joints was impaired, and parts of the tarsal region remained pseudostratified. (G) Overexpression of a moderate mC-RhoGAP68F caused tears of lateral cell-cell contacts and formation of spaces between cells (arrows). (H) The number of tears (arrows) was enhanced by expression of Rab7-GFP together with mC-RhoGAP68F.

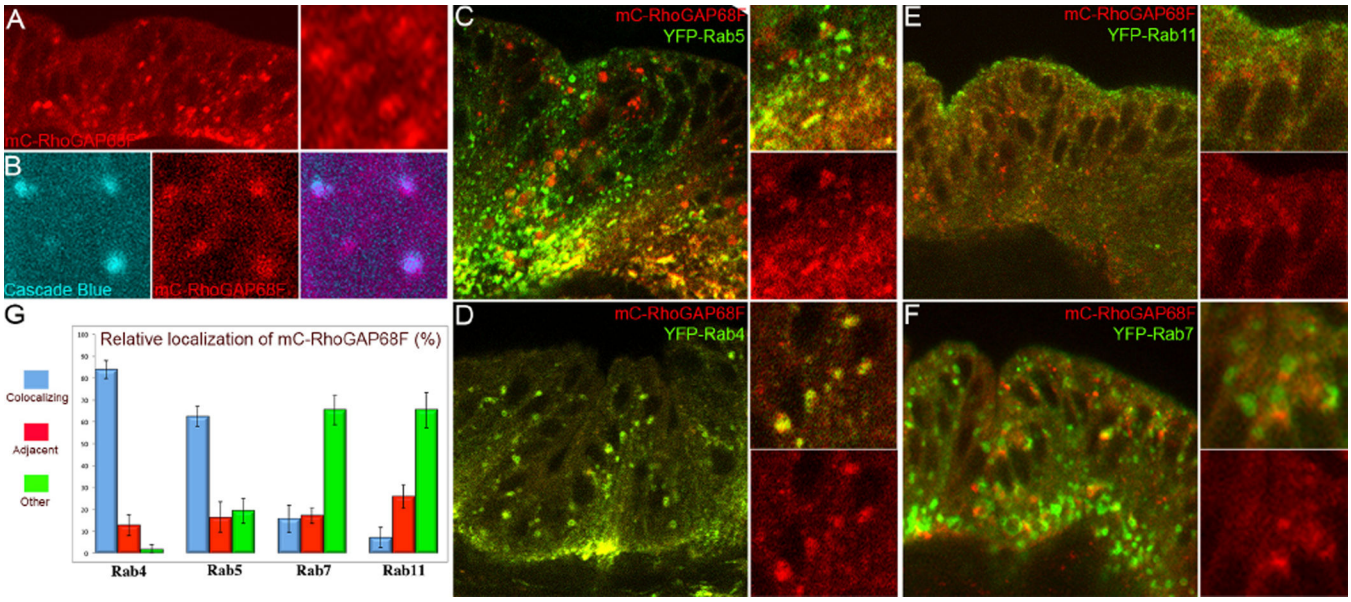

Figure 2.

RhoGAP68F localizes preferentially to Rab4 endosomes (A–B) Subcellular localization of a weak mCherry (mC)-RhoGAP68F expressed alone, or (C–G) together with fluorescently-tagged endosomal markers. (A) mC-RhoGAP68F localized to puncta and vesicles that (B) partially colocalized with fluorescent dextran (cascade blue) that was internalized from the cell surface by fluid phase endocytosis. (C–F) Analysis of mC-RhoGAP68F localization relative to endocytic markers revealed (C) moderate levels of coloclization with Rab5-GFP, (D) a near complete colocalization with YFP-Rab4, and lower levels of colocalization with (E) YFP-Rab11 and (F) Rab7-GFP. Note however that mC-RhoGAP68F and Rab7-GFP clearly localized to adjacent compartments in some regions (see inset). (G) Quantification of the localization of mC-RhoGAP68F relative to tagged Rab proteins. Bars represent Standard Deviations (S.D.) in all Figures. N=3 per genotype for the quantitative analysis; several hundreds endosomes were scored per sample.

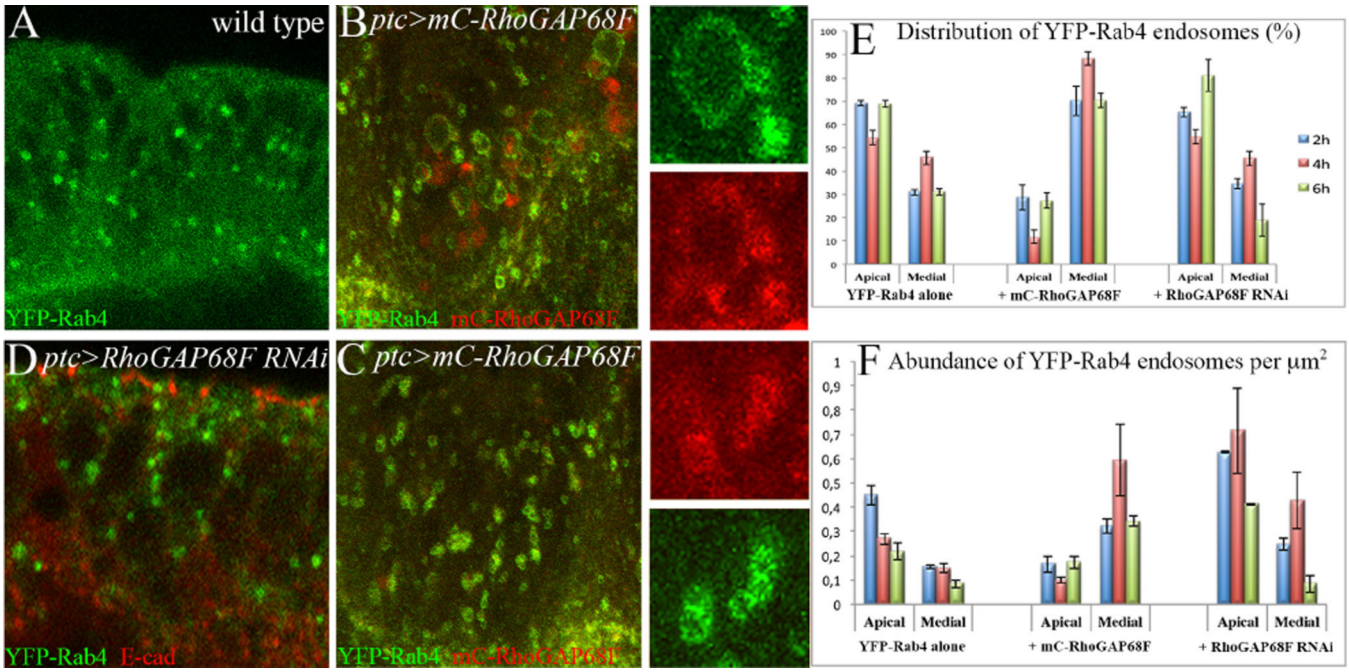

Figure 3.

RhoGAP68F affects the morphology and distribution of Rab4 endosomes along the epithelium apicobasal axis. (A) Localization of YFP-Rab4 in a wild type leg, (B–C) in a leg that overexpressed a moderate mC-RhoGAP68F protein, and (D) in a leg depleted for RhoGAP68F function. Overexpression of a moderate RhoGAP68F caused enlargement (inset in B) and clustering (inset in C) of Rab4 endosomes. (D) Depletion of RhoGAP68F increased the overall abundance of the Rab4 endosomes. (E–F) Quantification of the distribution and abundance of the Rab4 endosomes; wild type (average percentage of vesicles ± Standard Deviation (S.D.) at 2, 4 and 6h APF: 69%, 54% and 68% in the apical region compared to 31%, 46% and 32%, S.Ds. ± 1.8%, ± 2.9% and ± 1.43%, in the medial region, respectively); Overexpression of RhoGAP68F increased the abundance of the Rab4 endosomes in the medial region of the epithelium (to 71%, 88% and 73%; S.Ds. ± 5.4, ± 2.8 and ± 3.36, respectively, $p<0.001$ for all time points), and decreased their abundance in the apical region (to 29%, 12% and 27%, at 2, 4 and 6h APF). Depletion of RhoGAP68F increased the overall abundance of Rab4 endosomes and only moderately altered their distribution along the apicobasal axis at 6h APF (80% ± 6.76% compared to 70% ± 1.43% in wild type, $p<0.05$). N=3 per time point per genotype.

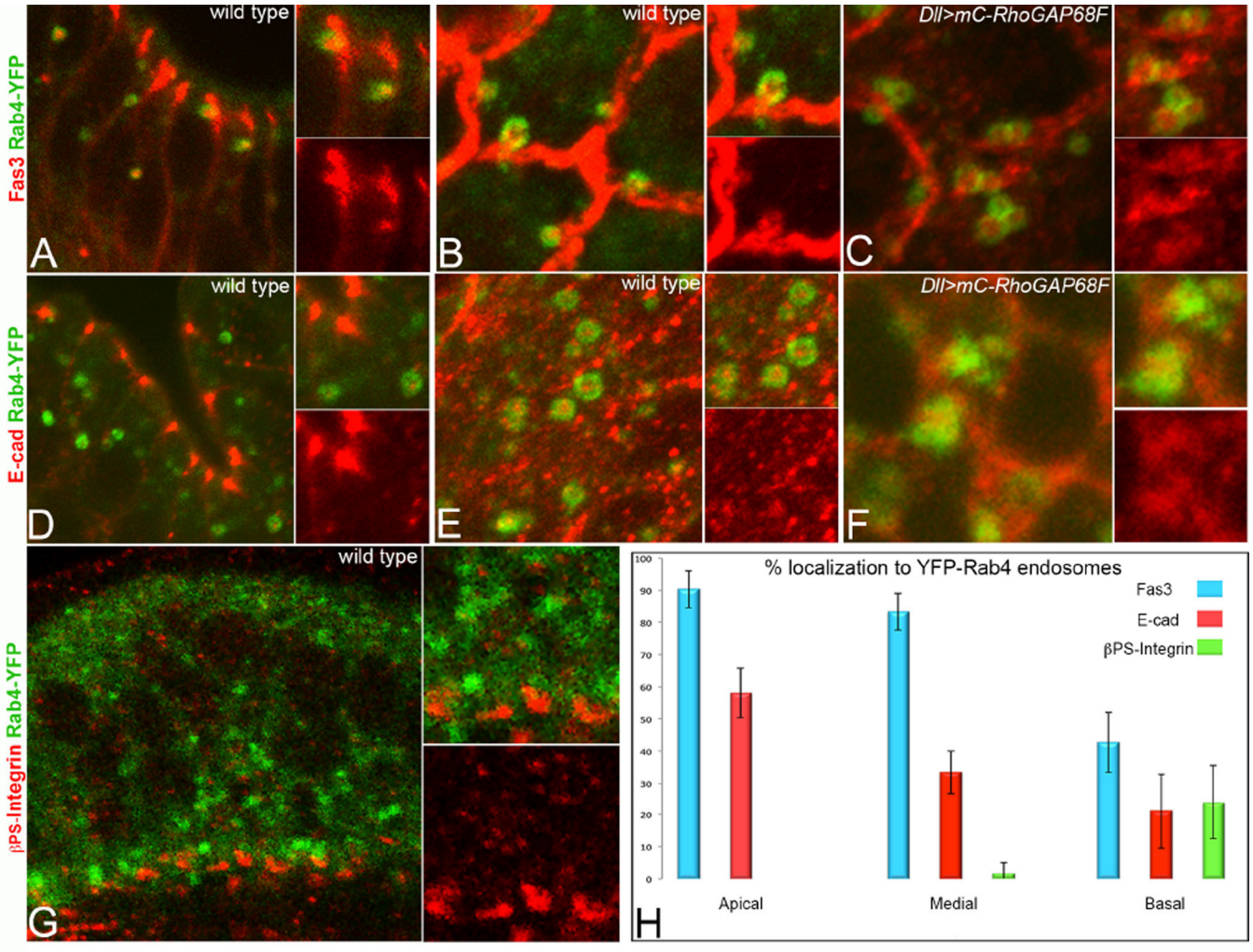

Figure 4.

The Rab4 endosomes return the adhesion receptors Fas3 and E-cad back to the cell surface. (A, D, G) Apicobasal and (B–C, E–F) planar sections across the tarsal region at 4h APF. (A–C) Fas3 and (D–F) E-cad accumulated at high level in Rab4 endosomes and Fas3 and E-cad were clearly seen in Rab4 endosomes in the process of fusing with the cell surface (B and data not shown). Overexpression of RhoGAP68F caused clustering of Rab4 endosomes containing the adhesion proteins (C) Fas3 and (F) E-cad. (G) βPS-Integrin accumulated at lower levels in Rab4 endosomes in the basal region of the epithelium. (H) Quantification of the relative accumulation of Fas3, E-cad and pPS-Integrin in the apical (above nuclei), medial (at the plane of nuclei) and basal (below nuclei) regions of the epithelium, respectively, at 4h APF. N=3 per each adhesion protein analyzed.

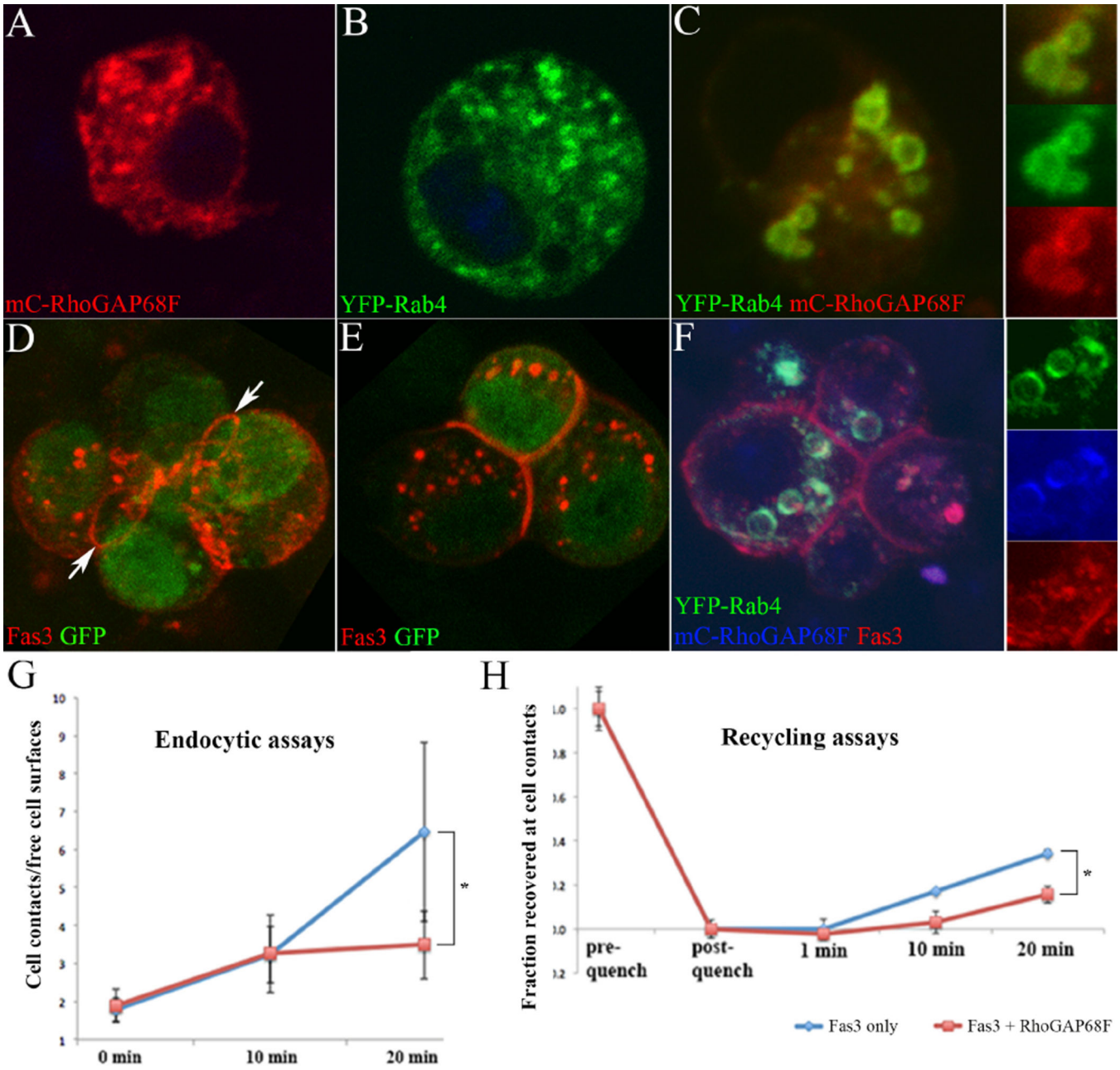

Figure 5.

RhoGAP68F inhibits the accumulation of Fas3 at cell-cell contacts. S2 cells expressing (A) mC-RhoGAP68F, (B) YFP-Rab4, (C) mC-RhoGAP68F and YFP-Rab4, (D–E) Fas3, and (F) YFP-Rab4, mC-RhoGAP68F and Fas3. Expression of RhoGAP68F together with Rab4 caused enlargement of the YFP-Rab4 endosomes (compare B with C). (D–E) Fas3 localized at high levels to a rim at contacts between cells (arrows), in puncta in the cytoplasm, and at free cell surfaces. (F) Expression of Fas3 together with YFP-Rab4 and mC-RhoGAP68F caused clustering and enlargement of YFP-Rab4/mC-RhoGAP68F endosomes that accumulated Fas3. (G) Endocytic assays revealed that Fas3 was endocytosed from the cell surface and moved to cell contacts, and that mC-RhoGAP6F significantly decreased Fas3

accumulation at cell contacts. Data represent the mean signal intensity at cell contacts divided by the mean signal intensity at free cell surfaces. We find that in cells expressing RhoGAP68F together with Fas3, the overall levels of Fas3 at free cell surfaces and cell contacts were significantly reduced by 23% and 27%, respectively, when compared with cells expressing Fas3 alone (mean signal intensity ± S.D.: 335.816 ± 78.445 compared to 259.494 ± 54.098 at cell contacts, $p<0.001$; 188.385 ± 53.44 compared to 137.755 ± 38.060 at free cell surfaces, $p<0.001$) likely as a result of Fas3 accumulating in Rab4 endosomes. (H) Recycling assays revealed that mC-RhoGAP68F significantly slowed the return of Fas3 to the cell surface. Data represent mean signal intensity at cell contacts after subtracting the mean pixel intensity remaining after quenching, divided by the mean pixel intensity at cell contact before quenching. N=15 per each condition per each time point, multiple contacts were analyzed per image. * $p>0.05$.

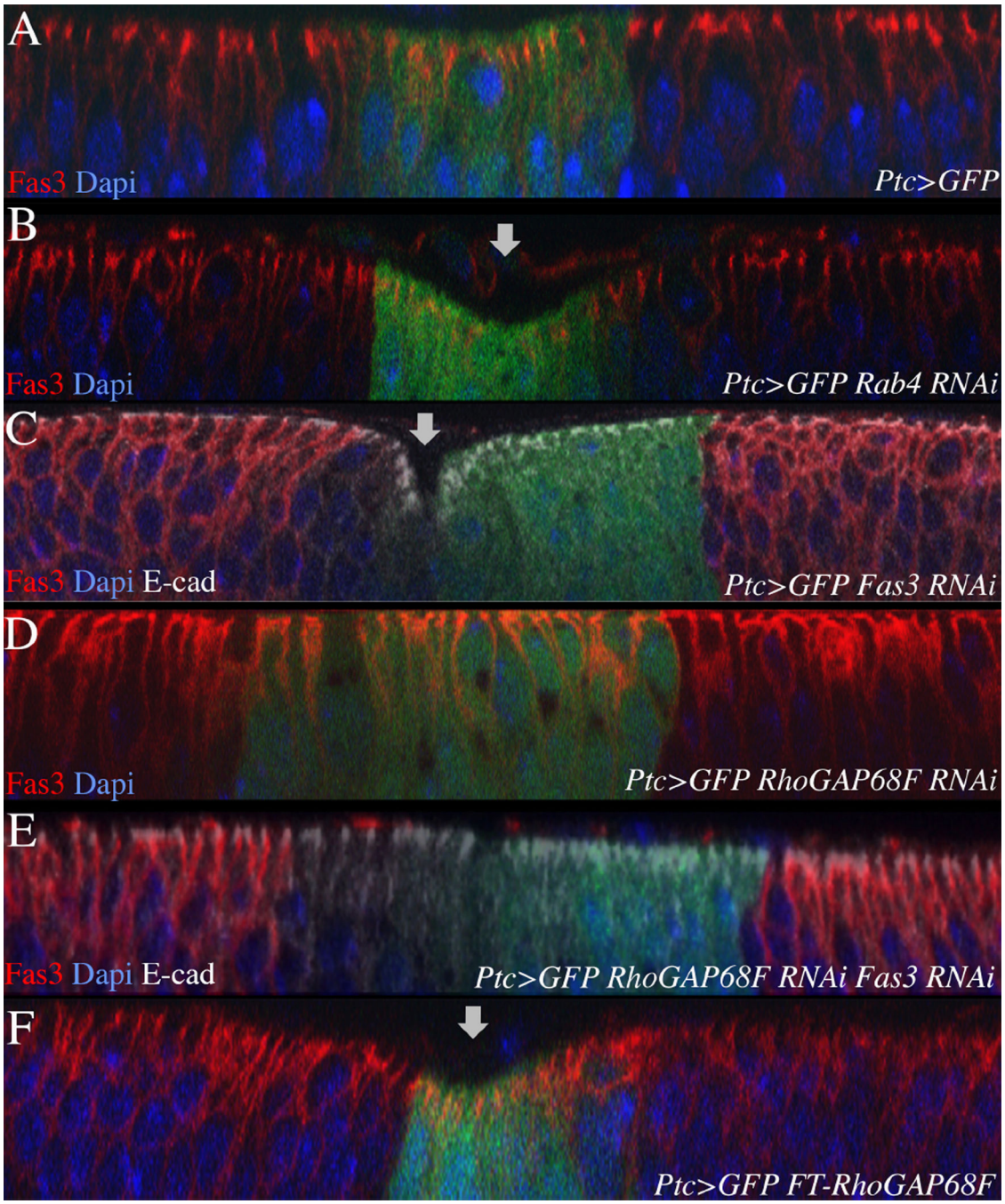

Figure 6.

RhoGAP68F and Fas3 interact genetically to affect epithelial morphology. (A) Expression of GFP in the Ptc domain had no effect on epithelial morphology. In contrast, (B) depletion of Rab4, or (C) Fas3, or (F) overexpression of Flag-RhoGAP68F caused bending of the epithelium in the Ptc domain. (D) Depletion of RhoGAP68F in the Ptc domain had no affect on epithelial morphology. (E) Strikingly, depletion both Fas3 and RhoGAP68F suppressed the bending of the epithelium promoted by depletion of Fas3 alone. This result suggests that RhoGAP68F affects epithelial morphology at least in part through the regulation of Fas3

levels and dynamics. 20 discs were examined per genotype; representative examples are shown.

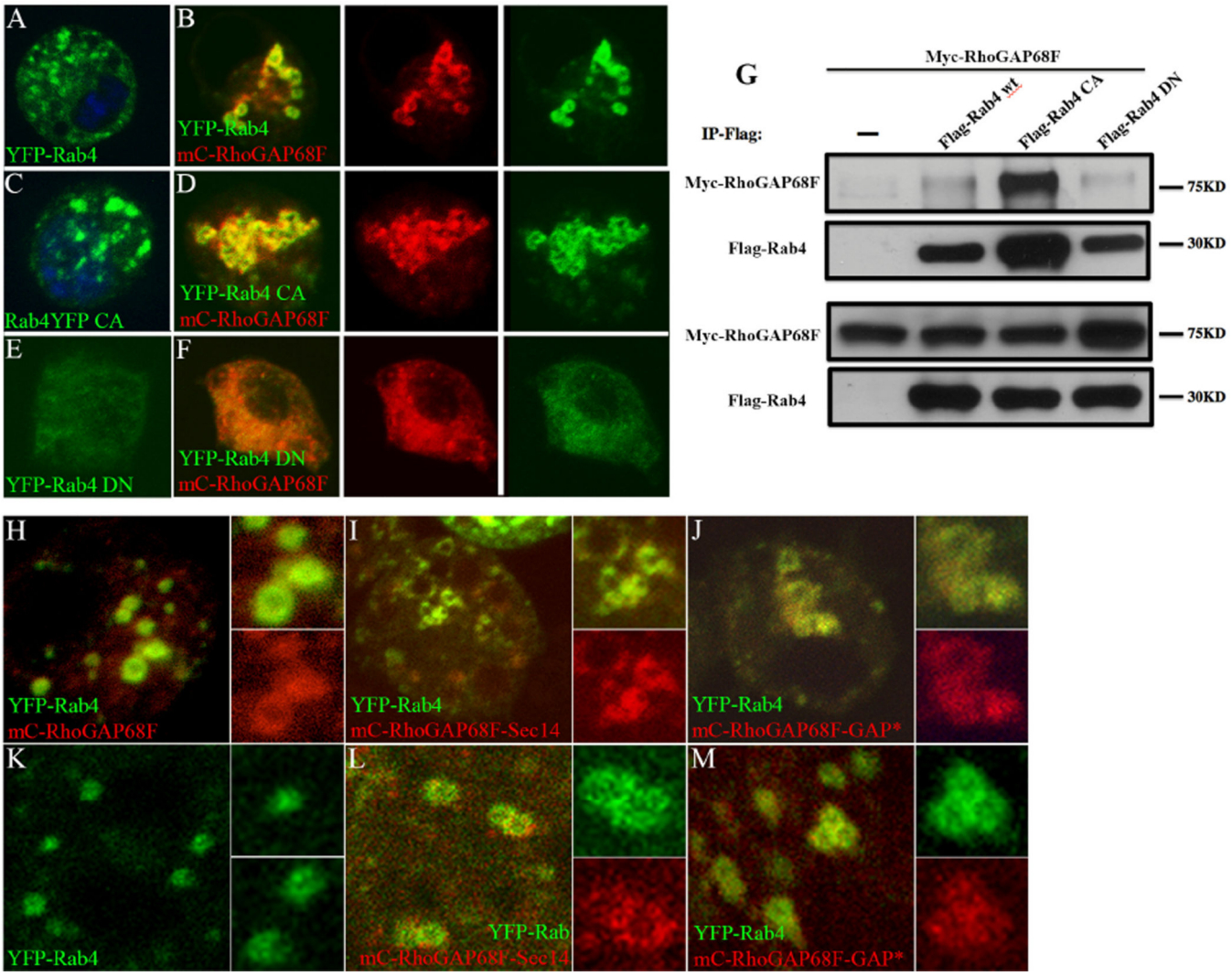

Figure 7.

RhoGAP68F interacts physically and preferentially with the active Rab4 protein and the RhoGAP68F–Sec14 domain localizes to Rab4 endosomes. (A–F) Localization and (G) physical interaction of RhoGAP68F with wild type, constitutively active and dominant negative YFP-Rab4 variants. (A) YFP-Rab4 localized to puncta in the cytoplasm. (B) Expression of mC-RhoGAP68F together with YFP-Rab4 caused clustering and enlargement of Rab4 endosomes. (C) Active YFP-Rab4 caused enlargement of the Rab4 endosomes, (D) Expression of mC-RhoGAP68F together with active YFP-Rab4 caused further enlargement and clustering of Rab4 endosomes and formation of extensive tubular structures. (E) Dominant negative YFP-Rab4 localized in a diffused pattern in the cytoplasm. (F) mC-RhoGAP68F expressed with the dominant negative Rab4 variant localized in a similar diffused pattern. (G) Co-IP assays revealed that the association of the RhoGAP68F protein was (~3.26 fold) stronger with the constitutively active Flag-Rab4 variant, and (~2.88 fold) weaker with the dominant negative variant compared to the association with the wild type tagged protein in a representative experiment. (H–M) Localization of mC-RhoGAP68F variants in S2 cells (H–J), and *in vivo* (K–M). A RhoGAP68F Sec14-only variant localized

to Rab4 endosomes both in S2 cells and *in vivo* (Fig. 7I, 7L). Similarly, a GAP deficient RhoGAP68F localized to the Rab4 compartment in S2 cells and *in vivo* (Fig. 7J, 7M). Both variants caused mild clustering and enlargements of the YFP-Rab4 endosomes (Fig 7I–J, L–M compared to H–K).